Adaptive-wavelet-filtering-based Stator Current Zero-crossing Detection Method for High-speed Micromotor

Zhang Chengbo,[1] Cui Yuguo,[1*] Li Jin-bang,[1] Liu Xiaoming,[1] Liu Kai,[2] and Lou Zhiwei[2]

[1]School of Mechanical Engineering and Mechanics, Ningbo University,
No. 818, Fenghua Road, Jiangbei District, Ningbo, Zhejiang 315210, China
[2]Ningbo WTOO Machinery and Technology Co., Ltd.
Phase 12, No. 139, Zhishufang North Road, Zhenhai District, Ningbo, Zhejiang 315211, China

The speed measurement of a high-speed micromotor often requires speed sensors, increasing the complexity and cost of the system. To solve this problem, a high-speed micromotor measurement method without a position sensor is proposed in this paper. A current probe is used to obtain the current signal of the high-speed micromotor. The collected signal is processed by adaptive wavelet filtering for noise reduction, and zero-crossing detection is used to calculate the frequency of the signal after noise reduction, so as to calculate the motor speed in real time. A photoelectric optical fiber sensor is used to verify the accuracy of motor speed measurement results. The results show that the difference between the speed measured by proposed method and the speed measured by the photoelectric optical fiber sensor is only 0.4%. This method is expected to be widely applied in the fields of motor performance detection and motor fault diagnosis.

1. Introduction

With the continuous progress and rapid development of science and technology, high-speed micromotors are playing an increasingly important role in aerospace,[1–3] medical devices,[4,5] precision machining,[6,7] and other fields. The stability of motor speed has a significant impact on system performance.

Motor speed is an important parameter of motor performance indicators, and changes in motor load, current, voltage, efficiency, and so forth affect the actual speed of a motor. At present, the commonly used motor speed measurement methods are mainly divided into synchronous measurement, counting measurement, and analog measurement. The synchronous measurement method uses the known frequency to measure the rotational speed synchronously with the rotation of the rotating body.[8] For example, a special power supply with an adjustable pulse frequency is added to a flash, so that the flash illuminates the rotating part of the motor fan. Then, the pulse frequency is adjusted so that the motor fan appears stationary. At this

moment, the pulse frequency is synchronized with the rotation frequency of the motor. The counting method calculates the rotational speed by counting pulses. Common pulse-generating devices include photoelectric encoders[8] and giant magnetoresistance sensors,[9] and there are different processing methods for pulse signals generated at different speeds. If the motor is operating at a high speed, then the frequency measurement method (M method) is used, which has a relatively low error at high speeds.[10] If the motor is operating at a low speed, the period method (T method) can be used, although the measurement accuracy decreases with increasing motor speed for the T method. If the motor speed is in a relatively wide range, a modified M/T method can be used to reduce the error by synchronizing the speed pulses and high-frequency counting pulses to the greatest extent possible.[11] The analog measurement method is an indirect method of measuring the motor speed that involves measuring physical quantities that change when the motor is rotating, for example, by analyzing the vibration signal, sound signal, and stator current signal of the motor to extract the frequency components of the speed from them and calculate the speed of the motor.[12] Although vibration detection technology has been used for a long time and the solution is mature, the disadvantages of the method are becoming increasingly apparent, such as the inconvenience of installing vibration sensors and the fact that the vibration signal is affected by mechanical resonance and machine noise during the measurement process. The use of an acoustic signal is a non-contact method for measuring motor speed, which also has the advantages of simple equipment, flexible sensor installation, and easy access to the signal.[13] However, the sound signal is easily affected by external interference. The motor stator current method is also a non-contact measurement method, in which the winding signal of the motor stator is collected by a current probe, and the collected current signal is analyzed spectrally to determine the motor speed.[14,15] This method can make up for the shortcomings of the traditional vibration and acoustic signal detection methods and can markedly reduce monitoring and detection costs.[16]

In analog measurement, the intermediate-frequency component of the collected signal is generally obtained to calculate the motor speed. Many methods are used for measuring the frequency of signals, among which the fast Fourier transform (FFT) method is used to solve the signal frequency; this method is not only stable and reliable but also accurate. However, if only the frequency of the collected signals is measured, there is no need to use such a complex and computationally expensive method as FFT. The zero-crossing detection method is a classical modulation domain analysis method. It has a simple principle and a convenient calculation process and is effective for modulation systems with a single carrier frequency and linear frequency modulation signals. However, for this method to be effective, the collected signals should not contain a large amount of noise interference.

To improve the frequency calculation accuracy of the zero-crossing detection method, it is necessary to denoise the collected signal. The Fourier transform is an essential method of analysis in the field of signal processing . However, it cannot effectively handle nonlinear signals, and there is a tradeoff between suppressing noise and protecting effective signals, which cannot meet the needs of noise reduction. With the progress of research, wavelet transform theory has been replacing the Fourier transform in the field of signal processing. The wavelet transform gives good time-frequency characteristics and can decompose signals of different

frequencies in non-stationary signals into non-overlapping frequency bands. It also has the advantages of local time-frequency characteristics, flexible selection of wavelet bases, and high calculation speed. Wavelet denoising can effectively remove noise, preserve the original signal, and improve the signal-to-noise ratio of the signal. In this paper, a motor speed measurement scheme based on motor stator current is proposed. First, the current signal of the motor stator winding is acquired by a current probe, then the adaptive wavelet transform is used to reduce the noise of the acquired signal, and the zero-crossing detection method is used to calculate the frequency of the noise-reduced signal. Finally, the motor speed is calculated using the frequency of the signal. The zero-crossing detection method is used to calculate the frequency of the motor stator winding signal, which is not only accurate, but also simplifies the calculation steps.

2.   Measurement Principle

2.1   Stator current method of speed measurement

Motor stator current analysis (MCSA) can not only measure motor speed but also diagnose motor faults.[17] In addition, it has two advantages. In addition, it has two advantages: 1) MCSA is simple to perform, as shown in Fig. 1, and only the stator winding wire of the synchronous motor must be placed in the current sensor during measurement. 2) MCSA has little effect on the motor itself and is a non-immersion method.

Therefore, in this study, the motor speed is measured by analyzing the spectral characteristics of the stator current signal. The motor speed in a synchronous motor is consistent with the rotating magnetic field generated in the stator winding of the motor; thus, the motor speed *n* can be obtained as follows by measuring the rotational speed of the rotating magnetic field:

$$n = \frac{60f}{p}. \tag{1}$$
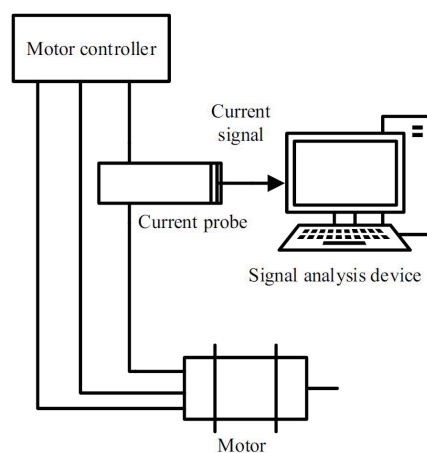
Fig. 1.   Schematic diagram of the current analysis method.

Here, p is the number of poles of the motor and f is the voltage frequency on the stator winding. When the motor is running, the motor wire stator winding passes through the front of the current probe and induces an electric potential inside the current probe. The current probe internally outputs an inverted compensation current that depends on the generated electric potential to make the magnetic field in the current probe zero. Therefore, the output compensation current frequency is the same as the actual current frequency.

2.2   Zero-crossing method of frequency measurement

From Eq. (1), the rotational speed of the motor is closely related to the frequency of the motor stator current signal. The frequency of the signal is usually calculated using FFT. However, when a large amount of data is processed by FFT, there is a lag due to the non-real-time treatment. Therefore, we need a method that can quickly and accurately detect the main frequency of the stator-induced current. The motor stator current signal is sinusoidal. The signal frequency can be derived by calculating the number of times the signal passes the zero point per unit time or the time difference between two adjacent points where the signal passes the zero point. Let two adjacent points be n_i and n_{i+1}, as shown in Fig. 2. If n_i is positive and n_{i+1} is negative, the number of lower crossing points in the signal is denoted *down*; conversely, the number of upper crossing points in the signal is denoted *up*. In a stator current signal with sampling time t, the frequency f of the stator current signal can be expressed as

$$f = \frac{n_{down} + n_{up}}{2} \times \frac{1}{t}, \tag{2}$$

where the sampling time t is expressed as

$$t = \frac{N}{f_s}. \tag{3}$$

Here, f_s is the sampling frequency of the digital signal and n is the length of the collected signal. We thus obtain

$$f = \frac{n_{down} + n_{up}}{2} \times \frac{f_s}{N}. \tag{4}$$

Compared with FFT, the zero-crossing method reduces the computational effort and improves the calculation speed of the signal frequency. However, the zero-crossing method requires a high signal-to-noise ratio for the acquired signal. If the signal is mixed noise, it directly affects the judgment of the zero-crossing method, resulting in differences between the measured and actual signal frequencies. Therefore, noise reduction is needed to improve the quality of the acquired signal frequencies.
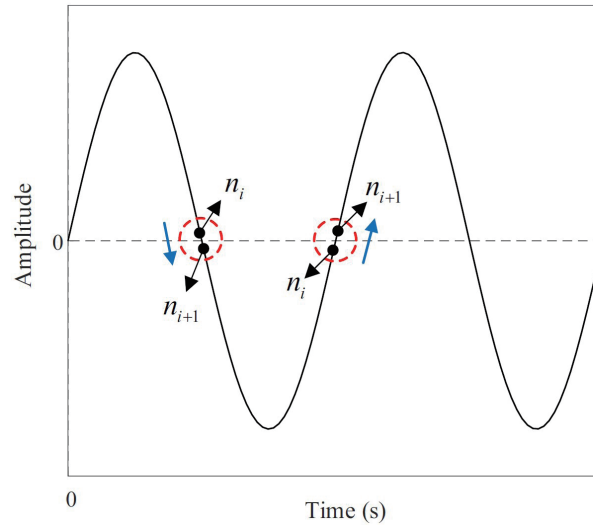
Fig. 2.　(Color online) Schematic diagram of zero-crossing detection method.

3.　Denoising of Stator Current Signal

In the actual measurement process, the accuracy of the zero-crossing method is decreased by the motor vibration and current noise superimposed on the signal collected by the current probe. Wavelet filtering has good time-frequency characteristics to focus signal details, and it can effectively filter out the noise of other frequencies superimposed on the measured signal frequency.[18] To reduce the noise interference, we designed a wavelet denoising algorithm with an adaptive threshold.

The hard threshold function is

$$\hat{w}_{j,k} = \begin{cases} w_{j,k}, & \left| w_{j,k} \right| \geq \lambda \\ 0, & \left| w_{j,k} \right| < \lambda \end{cases} \tag{5}$$

and the soft threshold function is

$$\hat{w}_{j,k} = \begin{cases} \operatorname{sgn}(w_{j,k})\left(\left| w_{j,k} - \lambda \right|\right), & \left| w_{j,k} \right| \geq \lambda \\ 0, & \left| w_{j,k} \right| < \lambda \end{cases} \tag{6}$$

where $w_{j,k}$ denotes the original wavelet coefficients, λ is the threshold, $\hat{w}_{j,k}$ denotes the wavelet coefficients obtained after intra-threshold function processing, and sgn( ) is a symbolic function that returns the positive and negative arguments.

The hard threshold function is discontinuous in the interval $[-\lambda, \lambda]$, and the reconstructed signal exhibits ringing and the pseudo-Gibbs phenomenon. The soft threshold function is continuous in the interval $[-\lambda, \lambda]$. However, when the mode is larger than the threshold λ, $w_{j,k}$ and

$\hat{w}_{j,k}$ always have a constant deviation, causing a difference between the reconstructed signal and the real signal. To choose the threshold function reasonably, we design a threshold function between the hard and soft threshold functions in this study. The adaptive thresholding function is

$$\eta(w_{j,k},\lambda,m_j) = \begin{cases} w_{j,k} - 0.5\,\text{sgn}(w_{j,k})\dfrac{\lambda^{m_j}}{\left|w_{j,k}\right|^{m_j-1}}, & \left|w_{j,k}\right| \geq \lambda \\[4mm] 0.5\,\text{sgn}(w_{j,k})\dfrac{\lambda^{m_j+1}}{\left|w_{j,k}\right|^{m_j}}, & \left|w_{j,k}\right| < \lambda \end{cases} \tag{7}$$

where m_j is a variable exchange value.

m_j can be a continuous real number greater than 1. When $m_j = 1$, the adaptive threshold function is very close to the soft threshold function. When $m_j > 10$, the function is very close to the hard threshold function. The adaptive threshold processing function obtains threshold functions suitable for wavelet coefficients at different scales by adjusting m_j, which is related to the energy at the scale of the wavelet decomposition.

$$m_j = 1 + 10\frac{E_{nj}}{E_{dj}} \tag{8}$$

Here, $m_j \in (1,11]$; when $j = 1$, $m_j = 11$, and as j increases, m_j decreases. $E_{n1} \approx \dfrac{1}{2^{j-1}}\sum\limits_{k=0}^{N-1} d^2_{1,k}$, $E_n \approx 2E_{n1}$, $E_{n,j} \approx \dfrac{1}{2^j}E_n \approx \dfrac{1}{2^{j-1}}\sum\limits_{k=0}^{N-1} d^2_{1,k}$, and $E_{d,j} = \sum\limits_{k=0}^{N-1} d^2_{1,k}$; D is the energy component of a high-frequency signal.

With increasing number of decomposition layers, the noise component of the wavelet coefficients decreases and the threshold value should decrease gradually. The fixed stratification threshold appears biased and cannot effectively handle wavelet coefficients on different decomposition layers. Therefore, an improved threshold is derived on the basis of the fixed threshold.

$$\lambda(j) = \frac{\sigma\sqrt{2\ln(N)}}{\ln(j+1)} \tag{9}$$

Here, j is the number of decomposition layers, but most of the noise is at the highest level, sub-high level, so $\tilde{\sigma}$ is as follows:

$$\tilde{\sigma} = \frac{\text{median}\left(\left|d_{j-1,k}\right|\right)}{0.6745}. \tag{10}$$

The processed wavelet coefficients are reconstructed by an inverse transform, and the filtered signal $s'(n)$ is obtained. White noise is superimposed on the sinusoidal signal to simulate the signal collected by the current probe, and the general and adaptive threshold function are separately used to denoise the analog signal. Figure 3 shows a comparison of the noise reduction effects of the hard and adaptive threshold functions.

It can be seen from the above analysis that the signal processed by the wavelet universal threshold denoising function has multiple transition points near the zero point, reducing the accuracy of the zero-crossing method. However, the signal processed by the adaptive threshold denoising function can effectively restore the original signal.

4.   Experimental Verification

4.1   Experimental system composition

Figure 4 shows the experimental device we used for measuring and verifying the speed of a high-speed micromotor. It consists of a miniature motor (LEXY F6), motor controller,
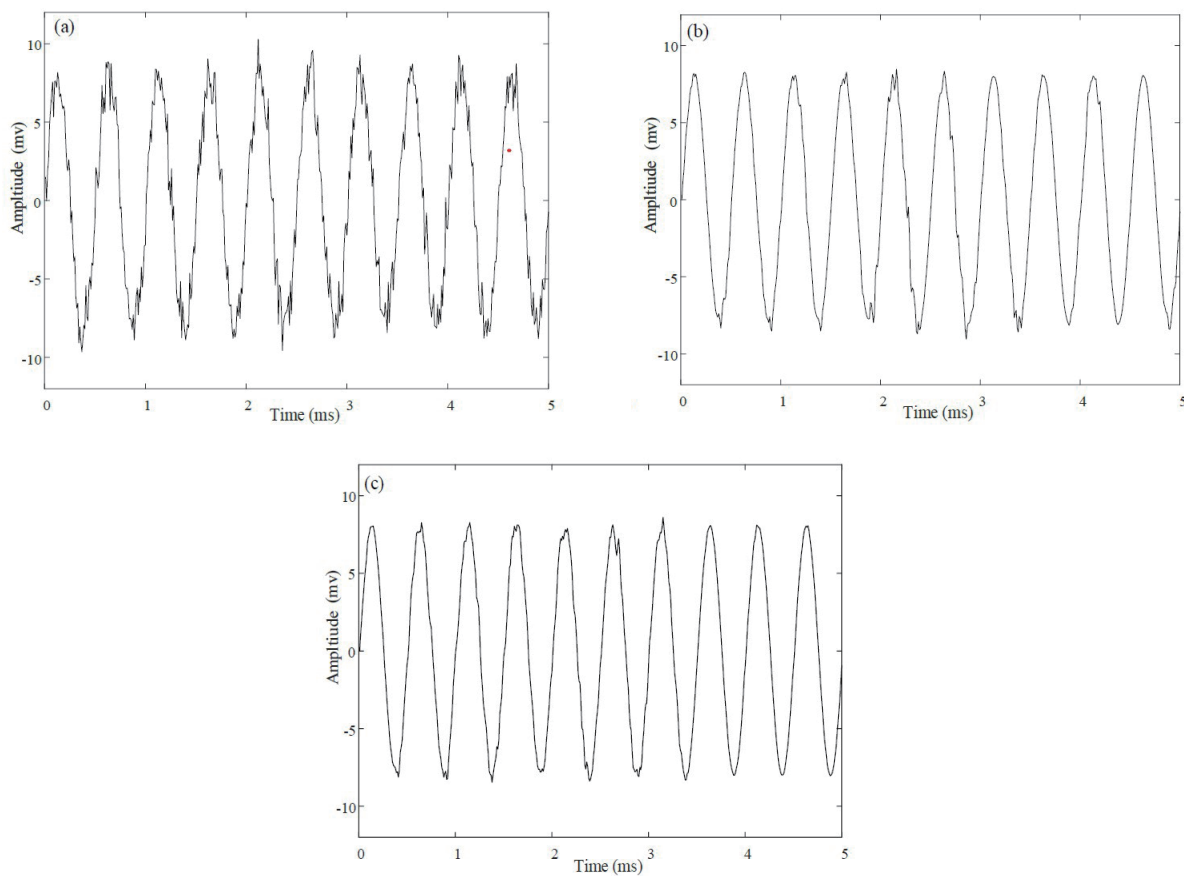
Fig. 3.   Wavelet threshold denoising simulation. (a) Original signal with white noise, (b) signal denoised by wavelet hard threshold function, and (c) signal denoised by adaptive threshold function.
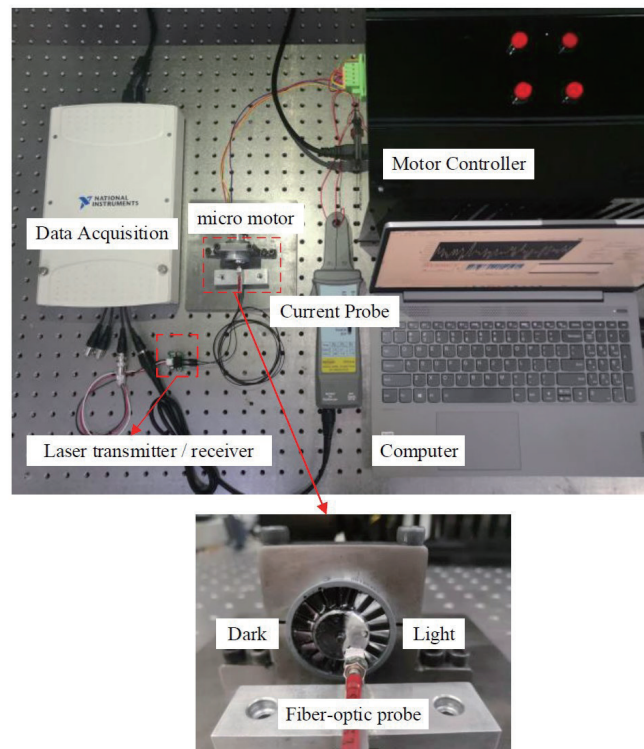
Fig. 4.   (Color online) Speed measurement and speed verification device for ultrahigh-speed micromotor.

multifunctional data acquisition card (National Instruments, PCI-6221), current probe (PT710-A), reflective laser sensor (lipoo NFRS-310), and computer. The experimental system consists of two parts, one for motor speed measurement and the other for motor speed verification measurement. The speed measurement process in the experiment is as follows. First, the computer sends a control signal to the motor driver, which causes the motor to rotate. Then, any wires in the motor stator winding pass through the induction loop of the current probe, and then the collected current signal is input into the computer through the acquisition card. After that, the signal noise is reduced by processing using adaptive wavelet filtering. Finally, the zero-crossing method is used to find the signal frequency after noise reduction and calculate the motor speed. To verify the method, the motor speed is measured by a reflective optical fiber sensor (response time 5 μs, maximum measurement speed 200000 rpm). The principle of the reflective laser sensor is that a laser emitted by a fiber probe is irradiated on the motor fan blade. When the laser is irradiated on the black part, the beam is absorbed, the sensor does not receive the reflected beam, and the sensor outputs a low level. Conversely, when the laser is irradiated on the reflective part, the beam is reflected, the sensor receives the reflected beam, and the sensor outputs a high level. The change between the high and low levels is transmitted to the computer by the acquisition card.

   In the speed test, the photoelectric method, zero-crossing detection method, and FFT were used to measure the speed of the motor under the same working condition. The zero-crossing

method and FFT obtained the signal frequency from the current signal, then the motor speed was calculated using Eq. (1).

4.2   Measurement results

The signal acquired by the current probe contains various kinds of noise, and the signal frequency cannot be accurately obtained using the zero-crossing method; thus, the acquired signal must be processed for noise reduction. In this study, we design an adaptive wavelet threshold denoising function to denoise the collected current signal. The signals are separately processed using the hard and adaptive wavelet threshold denoising functions, and the results are shown in Fig. 5.

By comparing the signal processing results of the two different wavelet threshold denoising functions, it is found that the signal denoising using the adaptive wavelet threshold denoising function method is more effective than that by wavelet threshold denoising.

We set up sampling data with different signal lengths and separately calculated the signal frequencies using FFT and zero-crossing detection to compare the processing ability and accuracy of the calculated frequencies of the two methods for different signal lengths.
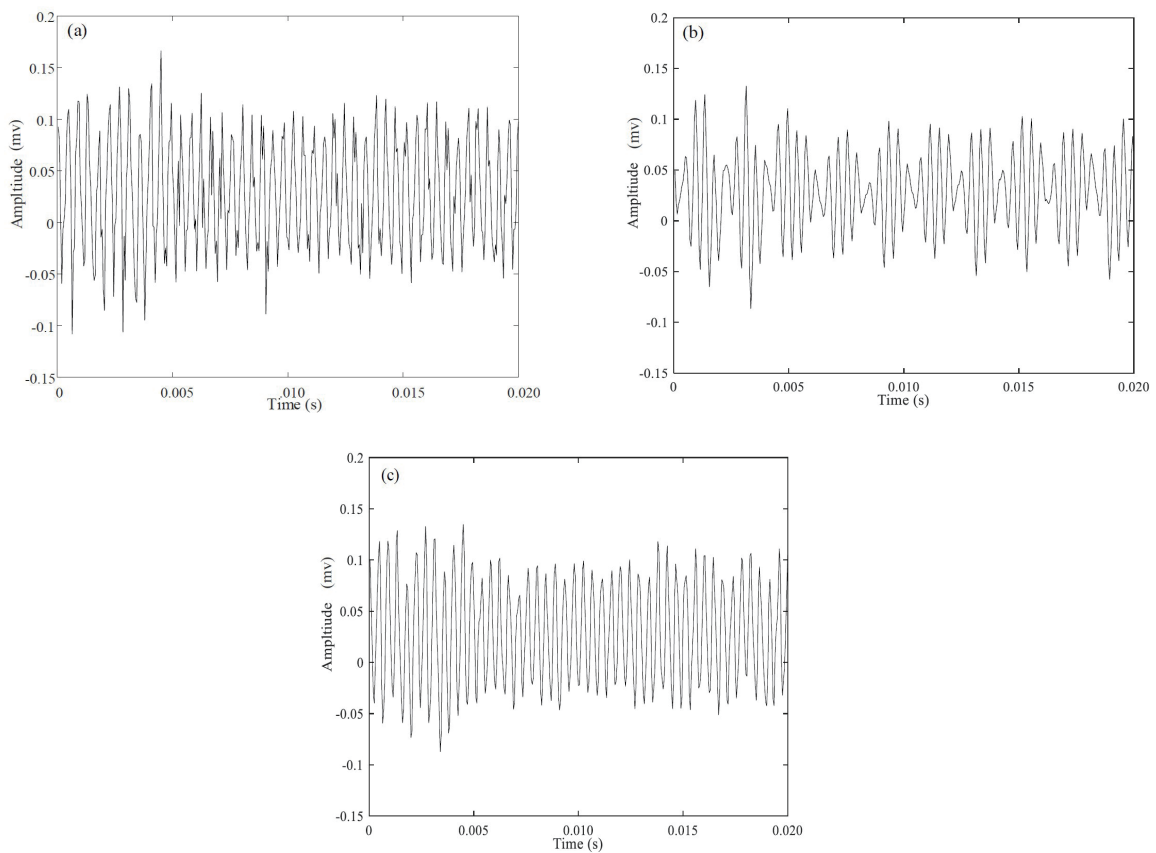
Fig. 5.   Signal measured by the current probe. (a) Original signal, (b) signal after hard wavelet threshold denoising, and (c) signal after adaptive wavelet threshold denoising.

As can be seen from Fig. 6, regardless of whether zero-crossing detection or FFT is used to calculate the frequency of the signal, there is a basic operation time. Taking a signal length of 0.05 s as an example, the algorithm using FFT to calculate the signal frequency takes about 0.72 s, whereas the algorithm using adaptive wavelet filtering and zero-crossing detection to calculate the signal frequency takes about 0.3 s. With increasing signal length, the processing time of the two methods also increases. When the signal length increases to 1 s, the time required for FFT to calculate the frequency is 0.83 s, whereas the time required for adaptive wavelet filtering and zero-crossing detection to calculate the frequency is only 0.41 s. These results show that for the same signal length, zero-crossing detection requires markedly less time than FFT.

Since the sampling frequency of the signal is 20 kHz, a small signal length may affect the accuracy of the frequency calculated by FFT. Figure 7 shows the calculated signal frequencies for different signal lengths.

As can be seen from Fig. 7, the signal frequency calculated by FFT tends to become stable with increasing signal length. However, the frequency calculated by the zero-crossing detection method always tends to be stable and does not change with increasing signal length. This shows that the zero-crossing detection method can accurately calculate the frequency of the signal even with a small number of sampling data points, whereas the FFT method requires a sufficient number of sampling points to accurately calculate the frequency of the signal.

In summary, calculating the signal frequency by the zero-crossing detection method has obvious advantages over calculation by the FFT method. From Fig. 7, when the signal length is 0.5 s, the total time required for adaptive wavelet noise reduction and zero-crossing detection is less than 0.5 s. Therefore, the speed refresh frequency is set to 2 Hz and the speed is set to 81200 r/min. Figure 8 shows a comparison of the motor speeds measured by the photoelectric method and calculated by the zero-crossing detection method.

From Fig. 8, the motor speed measured by the photoelectric method is similar to the set motor speed. Because the motor speed fluctuates within the allowable error range, the real-time speed of the detected motor is not a fixed value and belongs to the normal error range. It is found that
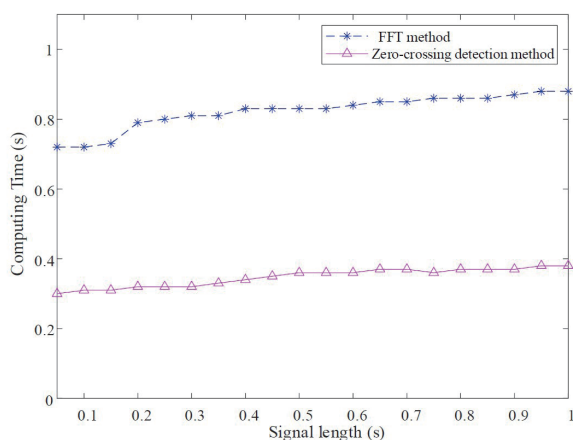
Fig. 6.   (Color online) Comparison of signal processing times for different signal lengths.
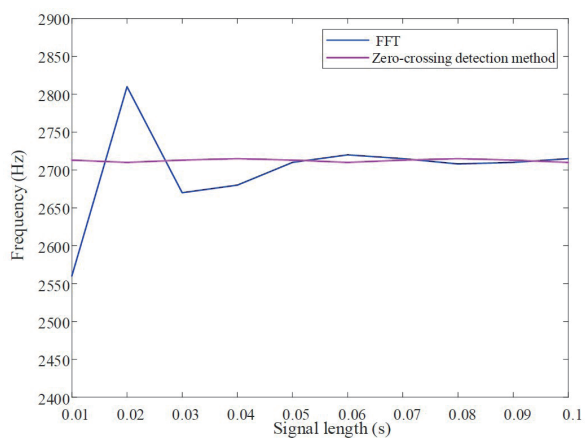
Fig. 7.   (Color online) Calculated signal frequencies for different signal lengths.
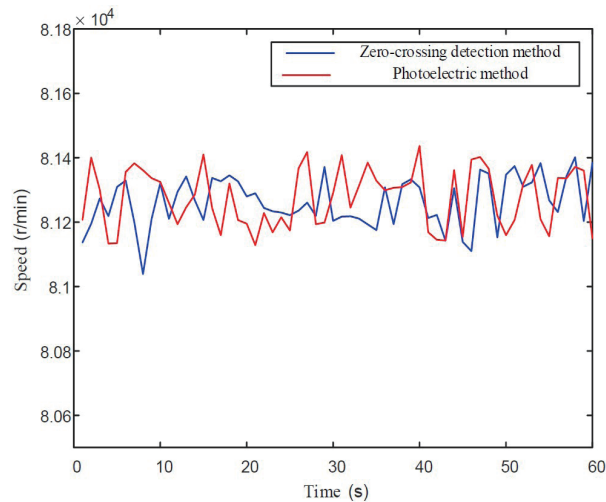
Fig. 8.   (Color online) Comparison of rotational speeds measured by different methods.

the rotation speed measured by the zero crossing detection method is similar to the rotation speed measured by the photoelectric method. The maximum difference is 316 r/min, and the relative error is less than 0.4% when the rotation speed is 81200 r/min.

5.   Conclusion

In this study, the motor stator current method is used to measure the motor speed. The motor stator current signal is first collected using a current probe and input to a computer through an acquisition card. Then, an adaptive wavelet filter is used to process the signal to reduce the noise. The frequency of the noise-reduced signal is measured using the zero-crossing detection method, from which the motor speed is calculated. Finally, the speeds measured by the zero-crossing detection, FFT, and photoelectric methods are compared, and experimental results show that the speed measured by the zero-crossing detection method has an error of only 0.4%. This method has promising applications for closed-loop motor control, motor performance testing, and fault analysis.

Acknowledgments

References

1   V. Madonna, G. Migliazza, P. Giangrande, E. Lorenzani, G. Buticchi, and M. Galea: IEEE Ind. Electron. Mag. **13** (2019) 4. https://doi.org/10.1109/MIE.2019.2936319
2   L. Gang, F. Jiancheng, and L. Jianzhang: Meas. Control. **41** (2008) 88. https://doi.org/10.1177/002029400804100305
3   J. Fu, Y. Fu, L. Yu, J. Guo, R. Yang, and M. Wang: Chin. J. Aeronaut. **31** (2018) 6. https://doi.org/10.1016/j.cja.2018.01.001

4　M. Juraeva, B. H. Park, K. J. Ryu, and D. J. Song: Int. J. Precis. Eng. Manuf. **18** (2017). https://doi.org/10.1007/s12541-017-0167-4

5　R. Holliday, S. Venugopal, A. Howell, and W. Keys: Br. Dent. J. **218** (2015) 23. https://doi.org/10.1038/sj.bdj.2015.40

6　I. Flur, V. Vyacheslav, K. Irek, and G. Denis: IECON 2016 42nd Annu. Conf. IEEE Industrial Electronics Society (IEEE, 2016). https://doi.org/10.1109/IECON.2016.7792986

7　P. Harris, B. Linke, and S. Spence: Procedia. CIRP **29** (2015) 29. https://doi.org/10.1016/j.procir.2015.02.046

8　C. Xiang, X. Wang, Y. Ma, and B. Xu: Math. Probl. Eng. **2015** (2015). https://doi.org/10.1155/2015/879581

9　P. P. Freitas, F. B. Silva, L. V. Melo, J. L. Costa, N. Almeida, and J. Bernardo: 1998 IEEE Int. Conf. Electronics (IEEE, 1998). https://doi.org/10.1109/ICECS.1998.813981

10　Y. Guo, J. Ma, and L. Li: The 2010 IEEE Int. Conf. Information and Automation (IEEE, 2010). https://doi.org/10.1109/ICINFA.2010.5512304

11　T. Tsuji, T. Hashimoto, H. Kobayashi, M. Mizuochi, and K. Ohnishi: IEEE Ttans. Ind. Electron. **56** (2008) 2. https://doi.org/10.1109/TIE.2008.2003208

12　S. Khanam, N. Tandon, and J. K. Dutt: Procedia Technol. **14** (2014) 14. https://doi.org/10.1016/j.protcy.2014.08.003

13　M. Amarnath and I. R. P. Krishna: IET Sci. Meas. Technol. **6** (2012) 4. https://doi.org/10.1049/iet-smt.2011.0082

14　R. Sabir, D. Rosato, S. Hartmann, and C. Guehmann: 2019 18th IEEE Int. Conf. Machine Learning and Applications (ICMLA) (IEEE, 2019). https://doi.org/10.1109/ICMLA.2019.00113

15　H.-W. Lee, D.-H. Cho, and K.-B. Lee: J. Power Electron. **21** (2021). https://doi.org/10.1007/s43236-021-00217-9

16　W. Li and C. K. Mechefske: J. Vib. Control. **12** (2006) 2. https://doi.org/10.1177/1077546306062097.

17　J.-H. Jung, J.-J. Lee, and B.-H. Kwon: IEEE T. Ind. Electron. **53** (2006) 6. https://doi.org/10.1109/TIE.2006.885131

18　X. Chert, J. Raja, and S. Simanapalli: J. Vib. Control. **1995** (1995) 2. https://doi.org/10.1016/0890-6955(94)p2377-r